

The Autonomous Cryocooled Sapphire Oscillator: A Reference for Frequency Stability and Phase Noise Measurements

This content has been downloaded from IOPscience. Please scroll down to see the full text.

2016 J. Phys.: Conf. Ser. 723 012030

(<http://iopscience.iop.org/1742-6596/723/1/012030>)

View [the table of contents for this issue](#), or go to the [journal homepage](#) for more

Download details:

IP Address: 82.225.18.231

This content was downloaded on 11/07/2016 at 14:58

Please note that [terms and conditions apply](#).

The Autonomous Cryocooled Sapphire Oscillator: A Reference for Frequency Stability and Phase Noise Measurements

V Giordano¹, S Grop², C Fluhr¹, B Dubois³, Y Kersalé¹, E Rubiola¹

¹ Dept TF, FEMTO-ST Institute, CNRS UMR 6174, Besançon, France

² Alemnis GmbH, Feuerwerkerstrasse 39, 3602 Thun, Switzerland

³ FEMTO Engineering, 32 avenue de l'Observatoire 25000 Besançon France

E-mail: giordano@femto-st.fr

Abstract. The Cryogenic Sapphire Oscillator (CSO) is the microwave oscillator which feature the highest short-term stability. Our best units exhibit Allan deviation $\sigma_y(\tau)$ of 4.5×10^{-16} at 1 s, $\approx 1.5 \times 10^{-16}$ at $100 \text{ s} \leq \tau \leq 5,000 \text{ s}$ (floor), and $\leq 5 \times 10^{-15}$ at one day. The use of a Pulse-Tube cryocooler enables full two year operation with virtually no maintenance.

Starting with a short history of the CSO in our lab, we go through the architecture and we provide more details about the resonator, the cryostat, the oscillator loop, and the servo electronics.

We implemented three similar oscillators, which enable the evaluation of each with the three-cornered hat method, and provide the potential for Allan deviation measurements at parts of 10^{-17} level. One of our CSOs (ULISS) is transportable, and goes with a small customized truck. The unique feature of ULISS is that its $\sigma_y(\tau)$ can be validated at destination by measuring before and after the roundtrip. To this extent, ULISS can be regarded as a traveling standard of *frequency stability*.

The CSOs are a part of the Oscillator IMP project, a platform dedicated to the measurement of noise and short-term stability of oscillators and devices in the whole radio spectrum (from MHz to THz), including microwave photonics. The scope spans from routine measurements to the research on new oscillators, components, and measurement methods.

1. Introduction

The Cryogenic Sapphire Oscillator (CSO) is the microwave oscillator which features the highest short-term stability. The Allan deviation (ADEV) $\sigma_y(\tau)$ is below 1×10^{-15} for integration time $\tau = 1-10^4$ s. Such stability enables the operation of laser-cooled microwave clocks at the quantum limit [1, 2]. The CSO proved to be useful at improving the resolution in Very Long Baseline Interferometry (VLBI) and in the deep-space networks for space-vehicle ranging and Doppler tracking [3, 4, 5, 6, 7, 8]. And it can enhance the calibration capability of Metrological Institutes, and help for the qualification of high performances clocks and oscillators [9].

2. History

Research on microwave sapphire Whispering Gallery mode (WG) oscillators started in our lab in 1995 with room-temperature and 77 K resonators. We developed several techniques to compensate for the high temperature sensitivity of the sapphire (70 ppm/K at 300 K) [10, 11]. At



the end of the 90s, CNES (the French space agency) and BNM (the French metrology agency, now LNE) encouraged us to develop a 4 K CSO for ground applications. We got help from the FSM lab at the University of the Western Australia (UWA) in a rather informal collaboration, still going on. Our first resonator was tested at UWA, and in 2001 we started the first liquid-He cooled resonator in Besançon [12]. In 2004 our open-cavity resonator achieved $\sigma_y(\tau) \leq 7 \times 10^{-15}$ at short term, and $< 2 \times 10^{-14}$ at one day [13, 14, 15].

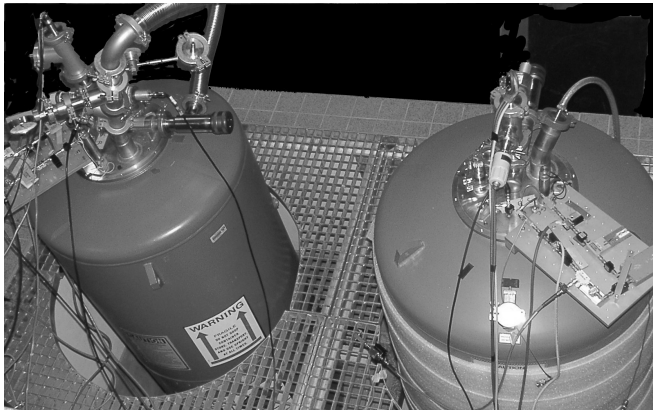


Figure 1. Liquid helium cryostats of the early CSOs at the Femto-ST Institute (2000).



Figure 2. 2014: The three CSOs of the Oscillator IMP platform.

The ELISA project, funded by the European Space Agency (ESA) started in 2007, with National Physical Laboratory (UK) and TimeTech GmbH (DE) as subcontractors. We demonstrated the first state-of-the-art frequency stability with an autonomous cryocooler. ELISA features $\sigma_y(\tau) \leq 3 \times 10^{-15}$ for $\tau = 1-10^4$ s [4, 5, 16, 17]. It was later moved to the ESA Deep Space Antenna Station DSA-3 in Malargüe, Argentina, where it is operational since.

In 2011, we designed a new CSO, codenamed ULISS, which can be transported with a small truck. In two years ULISS visited several European sites, traveling more than 10,000 km [18]. A set of three CSOs is now operational at our site. So, measuring ULISS before and after traveling, we can validate stability and spectral purity at destination. These CSOs have been used for example to check on the the stability of a laser stabilized on a ULE cavity, and to run with a cold atom fountain at SYRTE.

3. CSO Technology at FEMTO-ST

3.1. Architecture and Design

Frequency stability relies on the resonator, which is a cylinder of low-defect Al_2O_3 monocrystal. Al_2O_3 is chosen for lowest dielectric loss and good mechanical properties. The Whispering Gallery (WG) mode resonance provides the strongest confinement of energy inside the resonator, and in turn the highest quality factor Q . The unloaded Q of a 30–50 mm diameter, 10–30 mm high resonator exceeds 10^9 at 10 GHz and at liquid-He temperature. Industrial Al_2O_3 crystals show a useful turning point at 5–8 K due to impurities, detailed later.

The oscillator (Figure 3) is a Pound-Galani scheme [19], in turn derived from the Sulzer quartz oscillator [20]. In the Pound scheme [21], a voltage-controlled oscillator is frequency locked to the resonator using the reflected microwave to get the error signal. The Pound-Galani scheme differs in that the same resonator is also used as the reference of the locked oscillator. In our implementation, the resonator power is stabilized by a second control. Two tunnel diodes near the resonator input detect forward and reflected power.

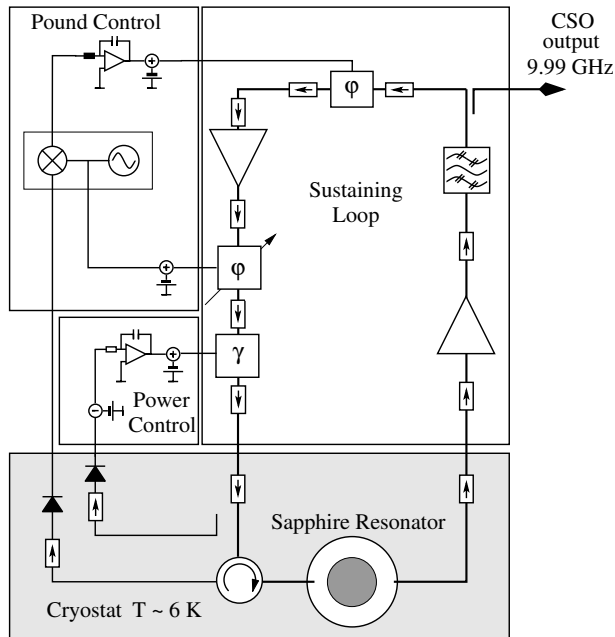


Figure 3. Oscillator main loop, with Pound and power servos.

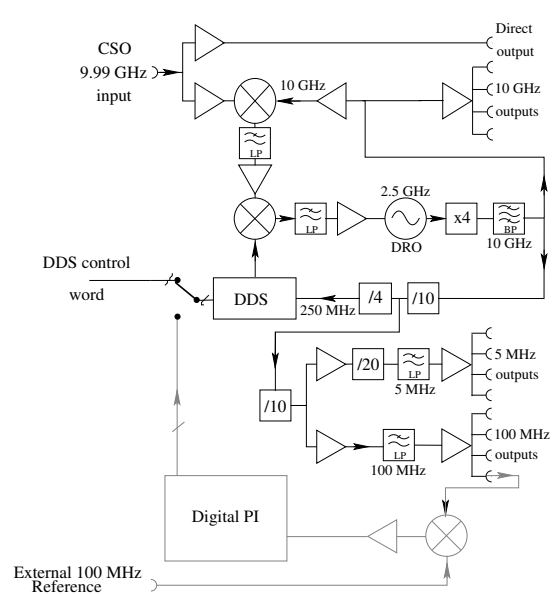


Figure 4. Low noise frequency synthesis for the generation of round frequencies: 10 GHz, 100 MHz and 5 MHz.

The complete machine includes a low-noise synthesizer which delivers 5–10–100 MHz and 10 GHz signals (Figure 4). The synthesizer can be frequency locked to a 100 MHz input, intended to discipline the CSO to a H maser for long term stability, letting the core oscillator unperturbed.

3.2. Resonator

As a general rule, the highest Q is expected from pure crystals with the lowest defect density. The problem with pure Al_2O_3 is that the the sensitivity of the resonant frequency to temperature is too high even at 4 K and monotonic. A turning point, necessary for stability, is provided by impurities. Paramagnetic ions as Mo^{3+} , Ti^{3+} Cr^{3+} substitute Al^{3+} and induce a small magnetic susceptibility χ . In the appropriate conditions, the thermal variation of χ compensates for the natural sensitivity of the sapphire, and the resonator sensitivity nulls at the turning-point temperature T_0 . The value of T_0 is specific to each crystal, as it depends on the concentration of dopants. However, a comfortable turning point just above 4 K has been found in most crystals grown with different methods, namely, Heat Exchange (HEMEX), Kyropoulos and Czochralski, and from different manufacturers. This is a fortunate outcome of technology. HEMEX grade sapphire proved to be the best choice for stability, as first demonstrated the UWA [22]. In [23] we demonstrate that crystals grown with the Kyropoulos or the Czochralski method can be used for short-term stability of 1×10^{-15} or better. A sketch of the resonator assembly, mounted in a copper cavity is shown in the figure 5. In our most implementations, the resonator has diameter of 54 mm and height of 30 mm, and it is operated in the $\text{WGH}_{15,0,0}$ mode, close to 10 GHz. Machining tolerance limits the accuracy to 5×10^{-5} , i.e., ± 5 MHz at 10 GHz. Hence we design the resonator for $\nu_0 = 10 \text{ GHz} - \delta_{\text{rf}}$, with $\delta_{\text{rf}} = 10 \pm 5$ MHz. In this way ν_0 is always lower than 10 GHz, and δ_{rf} is compensated by a DDS with a resolution $< 10^{-15}$. With $\delta_{\text{rf}} \lesssim 20$ MHz, the DDS stability and noise do not impact on the signal purity. Interestingly, machining tolerance guarantees the statistical independence of oscillators in a room by preventing microwave-leakage coupling. In fact, the frequency of two nominally equal resonators differ by 10^4 – 10^5 times the

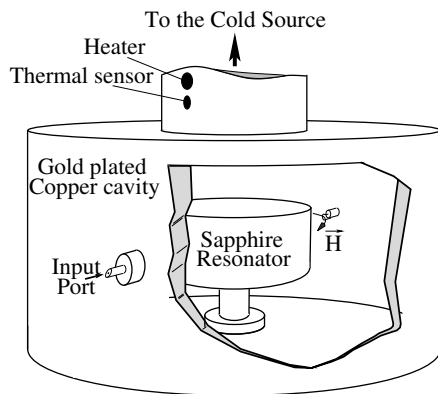


Figure 5. Sapphire resonator inside its Au-plated copper cavity. WGH-mode oriented loops provide external coupling (transverse magnetic field).

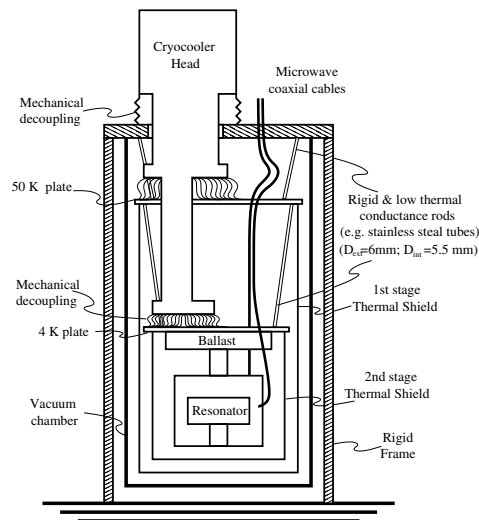


Figure 6. Scheme of the cryostat.

bandwidth.

3.3. Cryostat

The early CSOs were implemented in large liquid Helium Dewars (Figure 1). This setup is almost free from mechanical vibs, and provides good temperature uniformity. The main problem is refilling liquid He every 3 weeks. Since ELISA, we opted for a Pulse-Tube (PT) cryocooler because it can operate two years with no maintenance. Figure 6 sketches the principle our cryostats inspired from [24]. The 4 K plate that holds the resonator is rigidly coupled to the cryostat top flange by rigid rods. Conversely it is mechanically decoupled from the PT 2nd stage by means of a flexible thermal link made with OFHC copper braids. We tried some configurations using stainless steel tubes, fiber or even mylar for the rigid rods. The copper braids are made with 50 μm diameter OFHC copper wires. The number of wires and their length differ from one CSO to one other. The design criterium was to maintain the total equivalent thermal resistance below 10 K/W. Eventually we found the design of the mechanical suspension is not critical. For all the tested configurations a fractional frequency stability better than 1×10^{-15} at short-term can be obtained providing the other parts of the instrument are correctly tuned. We should notice that the typical displacement on the PT 2nd stage is *only* 24 μm peak-to-peak [25]. A reduction of the vertical vibrations to less than 1 μm rms is easily obtained by choosing the ratio between the stiffness of the rigid rods and those of the copper braids. A ratio of 100 can be easily obtained. The link's thermal resistance, combined with a ballast mass, low-passes the temperature fluctuations and enables stabilization better than within 100 μK .

3.4. Oscillator Electronics

The sustaining amplifier, based on commercial components at room temperature, compensates for the ≈ 30 dB loss of the resonator. Two low-noise amplifiers provide 54 dB gain. A Voltage Controlled Attenuator (VCA) controls of the power in closed loop. Two Voltage Controlled Phase Shifters (VCPS) are used for the Pound servo, for phase modulation and for frequency control. The first one is used to modulate the phase of the injected signal and the control signal is injected in the second one.

3.5. Pound Control

Thermal and mechanical fluctuations modulate the phase of the oscillator-loop path. This induces frequency noise through the Leeson effect [26], and in our case limits the stability to some 10^{-14} at $\tau = 1$ s. Random walk and drift makes the instability even worse at longer τ depending on the environment. These fluctuations are fixed with a Pound servo.

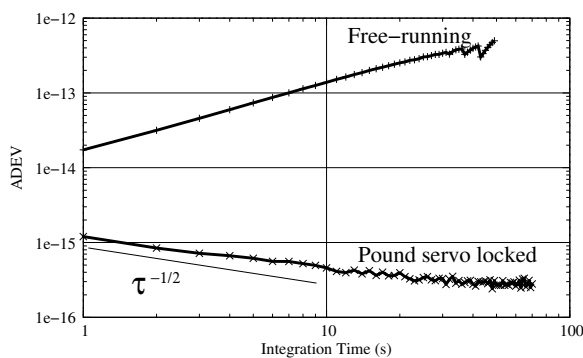


Figure 7. Allan standard deviation for a free and Pound-locked CSO.

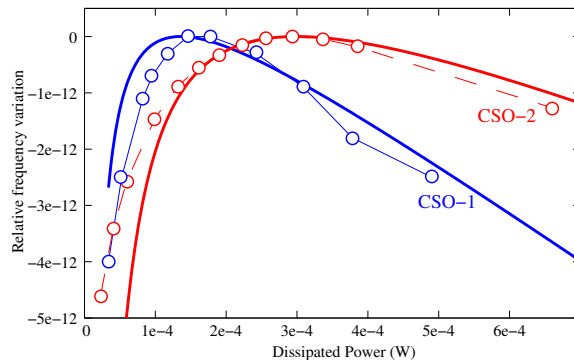


Figure 8. Power sensitivity of two resonators presenting different Q-factors.

A phase modulation at $\nu_m = 70$ kHz (typically) is applied at the input of the resonator, which has a bandwidth of ≈ 10 Hz. The tunnel diode DT1 beats the reflected carrier with the modulation sidebands. The DT1 signal output, down-converted from ν_m to dc, provides the error signal which is integrated and applied to the second VCPS, which controls ν_0 . The control bandwidth is of ≈ 1 kHz. The slope of the Pound discriminator is $D \approx 1 \times 10^{-3}$ V/Hz (typical). The noise measured at the output of DT1 at ν_m is $e_n \approx 10$ nV/ $\sqrt{\text{Hz}}$. Figure 7 shows the Allan deviation of a CSO in free-running and Pound-locked conditions. Here, $D \approx 7 \times 10^{-4}$ V/Hz. The expected stability is

$$\sigma_y(\tau) = \frac{e_n}{\sqrt{2}D\nu_0} \tau^{-1/2} \approx 1 \times 10^{-15} \tau^{-1/2}. \quad (1)$$

With a given noise in the loop, increasing D results in improved stability. However, below 1×10^{-15} other noise phenomena on the resonator become dominant.

3.6. Power Control

The CSO sensitivity to microwave power results from thermal effects and from the radiation pressure. The latter shows up at high Q . Beyond $300 \mu\text{W}$, the power shift is of the order of $1 \times 10^{-8}/\text{W}$. At lower power, the power shift is affected by the paramagnetic impurities for modes laying nearby or in the Electron Spin Resonance (ESR) bandwidth. A sweet point P_0 has been demonstrated at 10 GHz, where the effect of ESR saturation of Cr^{3+} ions compensates for the radiation pressure, and the overall power shift nulls [27] (Figure 8). Of course, this relaxes the specs for power stabilization.

4. Current Status

We have implemented three CSOs, which are a part of the Oscillator IMP project (Figure 2). They were assembled successively since 2012. They are in principle equal, but for the resonator and minors details. Two of them (CSO-1 and CSO-2) are equipped with a HEMEX crystal, the third one uses a Kyropoulos crystal. The main characteristics of each resonator are given in

Table 1. Resonator characteristics.

	CSO-1	CSO-2	CSO-3
Frequency ν_0 (GHz)	9.988	9.995	9.987
Material	HEMEX	HEMEX	Kyropoulos
Loaded Q-factor Q_L	1×10^9	350×10^8	400×10^8
Input coupling coeff. β_1	1	1	0.92
Turnover temperature T_0	6.238 K	5.766 K	6.265 K
Injected power	100 μ W	300 μ W	70 μ W

table 1. Only CSO-1 is fully optimized, CSO-2 and CSO-3 need an additional adjustment of the resonator coupling.

The individual stabilities are measured with the three-cornered hat method. The CSO output signals are mixed to obtain the three beatnotes: $\nu_{12} = 7$ MHz, $\nu_{13} = 0.9$ MHz and $\nu_{23} = 7.9$ MHz. These beatnotes are analysed using a multi-channels K&K-FXE SCR digital phase recorder [28]. The three channels work in parallel thereby the data acquisitions are synchronous. All datas are processed using the frequency average mode with one second averaging time (equivalent to a Λ windowing for $\tau = 1$ s). The Allan standard deviations (ADEV) are computed for the different integration times τ by grouping the 1-s data. The hypothesis of statistical independence is supported by the spectral separation of the core oscillators, and also by the independent temperature controls.

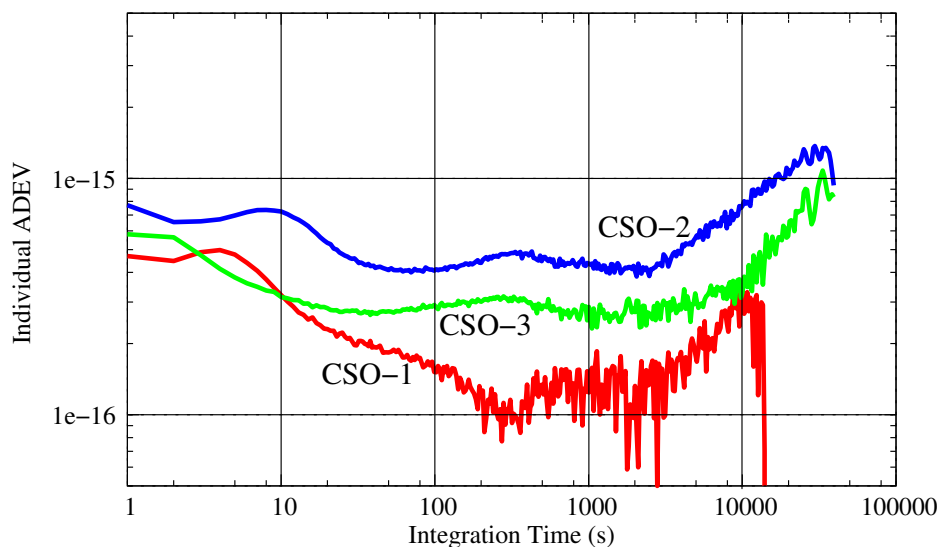


Figure 9. Individual ADEV from the 3-cornered-hat method.

At $1 \text{ s} \leq \tau \lesssim 50 \text{ s}$, the individual ADEVs roll off, but they do not follow the expected $\tau^{-1/2}$ law. The white FM noise due to the Pound discriminator is hidden under a bump at 10 s, most likely due to the 4-K temperature control. At longer τ , ADEV hits a floor, which is $\sigma_y(\tau) \approx 1.5 \times 10^{-16}$ at $100 \text{ s} \leq \tau \leq 5,000 \text{ s}$ for the best oscillator. The small bumps at 400 s match the fluctuation due to the on-off air conditioning system. In this region, there is some correlation between the units. Anyway, we are in the process of installing a new PI control which stabilizes room temperature and humidity.

Acknowledgments

This work is supported by the French ANR Programme d'Investissement d'Avenir (Oscillator IMP, First-TF and Refimeve+ projects in progress at the TF Departments of Femto-ST Institute and UTINAM). The authors would also like to thank the Council of the Région de Franche-Comté for its support to our projects and the FEDER (Fonds Européen de Développement Economique et Régional) for funding one CSO.

References

- [1] Santarelli G et al., 1999 *Phys. Rev. Lett.* **82** (23) 4619–22
- [2] Takamizawa A et al. 2014 *IEEE Transact. UFFC* **61** (9) 1463–69
- [3] Dick G J, Santiago D G and Wang R T 1995 *IEEE Transact. UFFC* **42** (5) 812–19
- [4] Grop S et al. 2010 *Rev. Sci. Instrum.* **81** (2) 025102
- [5] Grop S et al. 2011 *Electronics Letters* **47** (6) 386–88
- [6] Nand N, Hartnett J, Ivanov E and Santarelli G 2011 *IEEE Transact. MTT* **59** (11) 2978–86
- [7] Doleman S et al. 2011 *Pub. of the Astronomical Soc. of the Pacific* **123** (903) 582–95
- [8] Rioja M, Dodson R, Asaki Y, Hartnett J and Tingay S 2012 *The Astronomical J.* **144** (4) 121
- [9] Dolgovskiy V et al 2014 *Appl. Phys. B* **116** (3) 593–601
- [10] Kersalé Y, Vallet O, Vives S, Meunier C and Giordano V 2001 *Electronics Lett.* **37** (23) 1392–93
- [11] Kersalé Y, Vives S, Meunier C and Giordano V 2003 *IEEE Transact. UFFC* **50** (12) 1662–66
- [12] Bourgeois P Y, Kersalé Y, Bazin N, Chaubet M and Giordano V 2003 *Electronics Lett.* **39** (10) 780
- [13] Bourgeois P Y et al. 2004 *Electronics Lett.* **40** (10) 605
- [14] Bourgeois P Y et al. 2004 *IEEE Transact. UFFC* **51** (10) 1232–39
- [15] Giordano V et al. 2005 *Europ. Phys. J.: Appl. Phys.* **32** 133–41
- [16] Grop S et al. 2010 *Electronics Lett.* **46** (6) 420–22
- [17] Grop S et al. 2011 *IEEE Transact. UFFC* **58** (8) 1694–97
- [18] Giordano V et al. 2012 *Rev. of Sci. Instrum.* **83** (8) 085113
- [19] Galani Z et al. 1984 *IEEE Transact. MTT* **32** (12) 1556–65
- [20] Sulzer P 1955 *Proc. IRE* **43** (6) 701–07
- [21] Pound R 1946 *Rev. Sci. Instrum.* **17** (11) 490–505
- [22] Luiten A N, Mann A G and Blair D G 1993 *Electronics Lett.* **29** (10) 879–81
- [23] Giordano V, Fluhr C, Grop S and Dubois B 2016 *IEEE Trans. on MTT* **64** (1) 78–85
- [24] Ikushima Y et al. 2008 *Cryogenics* **48** (9) 406–412
- [25] Wang C and Gifford P E 2002 *AIP Conference Proceedings* **613** (1) 641–48
- [26] Rubiola E 2008 *Phase noise and frequency stability in oscillators* (Cambridge: Cambridge University Press)
- [27] Giordano V, Grop S, Bourgeois P Y, Kersalé Y and Rubiola E 2014 *J. Appl. Phys.* **116** (5) 054901
- [28] Kramer G and Klische W *Proc. of the 2001 IEEE Int. Frequency Control Symposium* 144–51